THE BELL SYSTEM TECHNICAL JOURNAL
Vol. 51, No. 10, December, 1972
Printed in U.S.A.

Performance and Stability of Schottky Barrier Mixers

By C. DRAGONE

(Manuscript received June 21, 1972)

We discuss the performance of a Schottky barrier diode as a mixer when the barrier of the diode is open-circuited at the harmonics $2\omega_o$, $3\omega_o$, *etc. of the pump frequency* ω_o. *Such a mixer is shown to be capable of arbitrarily high conversion gain provided*

$$\omega_c \geqq \eta\omega_o ,$$

where ω_c *is the cutoff frequency of the diode and* η *is a parameter that is typically less than* 6.25 *and approaches* 4 *under certain ideal conditions. It is shown that the limit imposed by the series resistance of the diode on the double-sideband noise figure of the mixer is given by*

$$F_m > \left(1 - \eta \frac{\omega_o}{\omega_c}\right)^{-1}.$$

An experiment is described at 1.25 GHz *on a room temperature mixer whose double-sideband noise figure* F_m *as a function of gain has a minimum of about* 0.7 *dB (for gain less than unity) and a maximum of about* 2.3 *dB (for high gain).*

I. INTRODUCTION

In the past five years the performance of microwave mixers has been substantially improved with the advent of high quality Schottky barrier diodes.[1] The noise figures obtained so far are better by a factor of approximately 2 than those obtained previously using point-contact diodes.[1-4] The ultimate microwave noise figure obtainable with these devices is not yet known, but there is reason to believe that, at room temperature, a figure well under 3 dB is possible.

Calculation in a previous article[5] showed that a Schottky barrier diode with suitable characteristics should have a noise figure well under 1 dB provided the barrier of the diode is open-circuited at the harmonics

$2\omega_o$, $3\omega_o$, etc. of the pump frequency ω_o. However, that calculation neglects the barrier capacitance and is therefore valid only at low frequency. The present purpose is to investigate the effect of the barrier capacitance. Three main assumptions are made: (*i*) the barrier of the diode is open-circuited at $2\omega_o$, $3\omega_o$, etc, (*ii*) the output frequency p of the mixer is very low with respect to ω_o, and (*iii*) the diode can be represented by an equivalent circuit discussed in Section II.

A mixer is commonly considered to be a linear transducer having finite maximum gain and a noise temperature ratio close to unity; the maximum gain is usually considered its most important attribute.[1] However, this picture is not valid in general for the mixer under consideration here. It will be shown that this mixer is potentially unstable if the cutoff frequency ω_c of the diode is sufficiently high with respect to ω_o. Thus its gain is unlimited, in the sense that it can be made arbitrarily high by appropriately choosing the terminations at the input, image, and output frequencies (i.e., at $\omega_o \pm p$ and p).

In a previous article[6] the mechanism responsible for instability in a mixer was discussed and necessary and sufficient conditions for unconditional stability were derived. These conditions, given in Section II, are used to determine the relation between mixer stability and mixer parameters. The main result is that a mixer is potentially unstable (i.e., that high gain is possible) if and only if

$$\omega_c \geqq \omega_o \eta, \tag{1}$$

where η is a parameter the value of which depends primarily on the breakdown voltage V_B of the diode. It is shown that $\eta \rightarrow 4$ as $V_B \rightarrow \infty$ and that typically

$$4 < \eta < 6.25. \tag{2}$$

The value η has important significance in connection with the noise performance of a mixer *at high gain* because the limit imposed by the series resistance of the diode on the ultimate noise performance is given by the inequality

$$F_m > \left(1 - \eta \frac{\omega_o}{\omega_c}\right)^{-1}, \tag{3}$$

where F_m is the double-sideband noise figure.

Following the analysis of Ref. 5, an experiment was undertaken to determine the performance obtainable from a mixer satisfying assumptions (*i*), (*ii*), and (*iii*). We designed such a mixer and measured its behavior as discussed in Section VI. It was, as expected, potentially unstable. The double-sideband noise figure as a function of gain was found to have a minimum value of 0.7 dB, occurring at a gain less than unity, and a maximum of about 2.3 dB, at high gain.

High gain in a mixer is no new phenomenon; it was demonstrated both theoretically and experimentally more than 20 years ago.[7] Since then, the effect of the barrier capacitance has been treated by several authors.[8-12] However, to the best of our knowledge, the effect of the barrier capacitance in a mixer satisfying assumption (*i*) has never been studied before. The amplifying ability is not a surprising property (Ref. 6), but good noise performance at high gain is perhaps unexpected.

II. PRELIMINARY CONSIDERATIONS

The equivalent circuit of Fig. 1 is assumed for the Schottky barrier diode; it consists of a small series resistance R_s and two nonlinear elements, the barrier capacitance $C(v_b)$ and the barrier resistance $R(v_b)$. The capacitance $C(v_b)$ and the current i_R through $R(v_b)$ are assumed to obey the familiar relations

$$C(v_b) = \frac{C_0\sqrt{\phi}}{\sqrt{\phi - v_b}} \tag{4}$$

and

$$i_R = i_S\left[\exp\left(\frac{qv_b}{kT}\right) - 1\right], \tag{5}$$

where ϕ is the contact potential, i_S the saturation current, q the electronic charge, k the Boltzman constant, and T the absolute temperature; $q/kT \cong 40$ for $T \cong 290°K$.

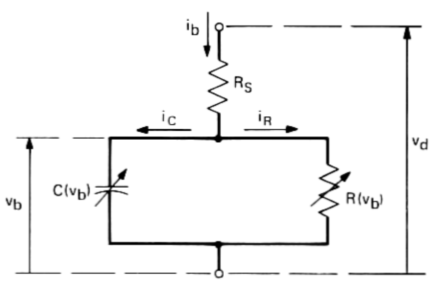

Fig. 1—Schottky barrier diode.

Figure 2 shows a two-terminal-pair network M driven by a sinusoidal current

$$i(t) = 2I \cos \omega_o t \tag{6}$$

and a direct current I_o. This network consists of the diode and two filters F_o and F_{ω_o}. According to assumption (*ii*), we assume for F_o and F_{ω_o} the following characteristics at the harmonics of ω_o (and in their vicinity): F_o is a short circuit at dc and an open circuit at ω_o, $2\omega_o$, $3\omega_o$, etc.; F_{ω_o} is a short circuit at ω_o and an open circuit at dc, $2\omega_o$, $3\omega_o$, etc. From Fig. 2 the terminal current of the diode is

$$i_b(t) = I_o + i(t). \tag{7}$$

The voltage v_b across the barrier is assumed periodic with frequency ω_o,

$$v_b(t) = v_{bo} + 2 \operatorname{Re} (V_{b1} e^{j\omega_o t} + \cdots), \tag{8}$$

where the dots indicate components at $2\omega_o$, $3\omega_o$, etc. Let Z_b denote the impedance presented by the barrier at ω_o.

$$Z_b = R_b + jX_b = \frac{V_{b1}}{I}. \tag{9}$$

Then the impedance Z presented by the network at ω_o is

$$Z = R + jX = R_S + Z_b. \tag{10}$$

The terminal voltage at dc is

$$V_o = V_{bo} + R_S I_o. \tag{11}$$

When this network (designated here by M; see Fig. 2) is used as a

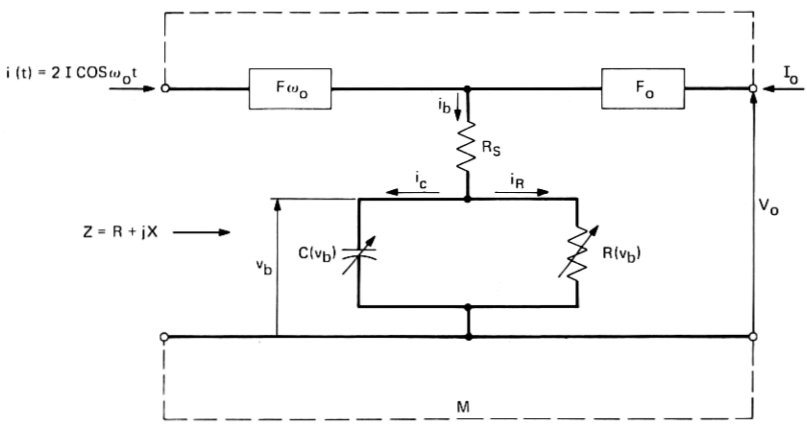

Fig. 2—Network M representing the mixer.

mixer, a small signal is applied at the input frequency $\omega_o + p$ (or $\omega_o - p$) and suitable terminations are provided at the image and output frequencies $\omega_o - p$ (or $\omega_o + p$) and p. Signal power then flows out of the network at $\omega = p$ to the output termination. The conversion gain, which is defined* here as the ratio of the output power to the power available from the input signal generator, has a finite maximum value only if M is unconditionally stable. If M is *not* unconditionally stable (i.e., if M is potentially unstable), its gain can be made arbitrarily high by properly choosing the terminations at $\omega_o \pm p$ and p. To determine the conditions for which M is potentially unstable, we assume $p \ll \omega_o$ [assumption (*ii*)]; this allows us to use the stability criteria of Ref. 6, which are discussed in the following part of this section. Since application of these criteria does not require a knowledge of the conversion properties of M at $\omega_o \pm p$ and p, the analysis will be concerned exclusively with the behavior of M at ω_o and dc.

2.1 *Stability Criteria*[6]

Let a one-terminal-pair network be constructed by connecting M to a dc source as shown in Fig. 3. The nonlinear impedance Z characterizing the terminal behavior at ω_o of this network is a function of the amplitude I of $i(t)$. The form of this function depends upon the characteristics of the dc source. Of particular interest are the two cases arising when the dc source is: (*i*) an ideal current source with infinite internal impedance, or (*ii*) an ideal voltage source with zero internal impedance. It has been shown in Ref. 6 that a necessary and sufficient condition for the network M to be potentially unstable is

$$4R \frac{d(IR)}{dI} \leqq \left(I \frac{dX}{dI}\right)^2 \tag{12}$$

in one of the above two cases.†

The network M imposes a set of nonlinear relations between its terminal voltages and currents at dc and ω_o. Because of these relations, the impedance Z and the dc voltage V_o can be regarded as functions of I_o and I,

$$R = R(I_o, I), \qquad X = X(I_o, I)$$
$$V_o = V_o(I_o, I). \tag{13}$$

* There are several ways of defining the gain of a mixer. A different definition will be used [see eq. (51)] in connection with the experiment described in Section VI, where the input signal generator will contain both $\omega_o + p$ and $\omega_o - p$. However, the particular definition is immaterial to the analysis.

† For the network of Fig. 2 one can show that $R > 0$ and $\partial V_o/\partial I_o > 0$; if these two inequalities are not satisfied, the network would obviously be potentially unstable.

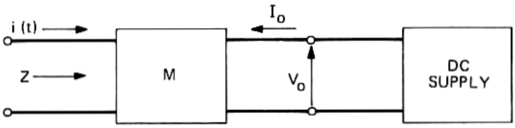

Fig. 3—Mixer connected to a dc bias supply.

These three functions completely describe the terminal behavior of M. If these functions are known, the derivatives appearing in inequality (12) can be evaluated as follows.

Note first that the two cases mentioned above correspond to the two conditions

$$I_o = \text{constant}, \tag{14}$$

$$V_o = \text{constant}. \tag{15}$$

Thus, in the former case, inequality (12) takes the form*

$$4R \frac{\partial(IR)}{\partial I} \leqq \left(I \frac{\partial X}{\partial I}\right)^2, \tag{16}$$

involving only partial derivatives of $IR(I_o, I)$ and $X(I_o, I)$ with respect to I.

In the latter case, differentiating eq. (15) we obtain

$$dI \frac{\partial V_o}{\partial I} + dI_o \frac{\partial V_o}{\partial I_o} = 0.$$

Thus,

$$\frac{dI_o}{dI} = -\frac{\partial V_o}{\partial I}\left(\frac{\partial V_o}{\partial I_o}\right)^{-1}.$$

Using this relation and the rule

$$\frac{d}{dI} = \frac{dI_o}{dI}\frac{\partial}{\partial I_o} + \frac{\partial}{\partial I},$$

we obtain for inequality (12)

$$4R \frac{\partial V_o}{\partial I_o}\left[\frac{\partial V_o}{\partial I_o}\frac{\partial(IR)}{\partial I} - \frac{\partial V_o}{\partial I}\frac{\partial(IR)}{\partial I_o}\right] \leqq \left[I \frac{\partial X}{\partial I}\frac{\partial V_o}{\partial I_o} - I \frac{\partial X}{\partial I_o}\frac{\partial V_o}{\partial I}\right]^2. \tag{17}$$

Inequalities (16) and (17) will be useful in Section IV.

* Throughout this paper $\partial/\partial I_o$ (or $\partial/\partial I$) is used to indicate differentiation with I (or I_o) held constant.

In the following section we consider the behavior of M in a limiting case and find that a simple relation exists between Z and V_o, I. Because of that relation, it is possible to ascertain stability directly from inequality (12), rather than using (16) and (17).

III. ANALYSIS OF A LIMITING CASE

Analysis of the circuit of Fig. 2 is a considerable task, primarily because the current i_c through $C(v_b)$ is not in general simply related to the total current i_b through the barrier. However, if the frequency ω_o is sufficiently high, the current i_R absorbed by $R(v_b)$ is much smaller than i_c for all t, and i_c is approximately equal to the alternating component of i_b.

$$i_c(t) \cong 2I \cos \omega_o t. \tag{18}$$

In the present section we study this case. Our main result is inequality (37).

If q and S denote the charge and elastance of the barrier capacitance respectively, then, since $S = dv_b/dq$ and $i_c = dq/dt$, we can write

$$\frac{dS}{dt} = \frac{dS}{dv_b}\frac{dv_b}{dq}\frac{dq}{dt} = \frac{1}{2}\frac{d[S^2]}{dv_b}\, i_c\, . \tag{19}$$

From eq. (4) and the fact that $S = C^{-1}(v_b)$,

$$S^2 = \frac{\phi - v_b}{(C_o\sqrt{\phi})^2}. \tag{20}$$

Taking the derivative and substituting in eq. (19) results in

$$\frac{dS}{dt} = -\frac{1}{2(C_o\sqrt{\phi}^{\,2}}\, i_c\, . \tag{21}$$

From this equation the alternative component of the elastance $S(t)$ produced by the current $i_c(t)$ of eq. (18) is determined. If S_o denotes the average value of $S(t)$, using eqs. (18) and (21),

$$S(t) = S_o + \frac{1}{(C_o\sqrt{\phi})^2}\left[\frac{jI}{2\omega_o}e^{j\omega_o t} - \frac{jI}{2\omega_o}e^{-j\omega_o t}\right]. \tag{22}$$

Substituting this equation in eq. (20) results in

$$v_b(t) = \phi - (C_0\sqrt{\phi})^2 S_o^2 - \frac{I^2}{(C_0\sqrt{\phi})^2 2\omega_o^2} + \left(-j\frac{S_o}{\omega_o}Ie^{j\omega_o t} + j\frac{S_o}{\omega_o}Ie^{-j\omega_o t} + \cdots\right), \tag{23}$$

where the dots indicate components at $\pm 2\omega_o$. The amplitudes of $v_b(t)$ at dc and ω_o, obtained from (23), are

$$V_{bo} = \phi - (C_o\sqrt{\phi})^2 S_o^2 - \frac{I}{(C_o\sqrt{\phi})^2 2\omega_o^2} \tag{24}$$

and

$$V = -j\frac{S_o I}{\omega_o}. \tag{25}$$

Thus, the reactance X presented by the barrier capacitance at ω_o can be written

$$X = -\frac{S_o}{\omega_o}. \tag{26}$$

From eq. (24)

$$S_o = \frac{1}{C_o\sqrt{\phi}}\sqrt{\phi - V_{bo} - \frac{I^2}{(C_o\sqrt{\phi})^2 2\omega_o^2}}. \tag{27}$$

Equations (26) and (27) specify the reactance X in terms of the two independent variables I and V_{bo}.

We now make the assumption that the diode is so operated that the power* absorbed by $R(v_b)$ at ω_o is much smaller than the power dissipated in R_S at ω_o. Because of this assumption, which is consistent with eq. (18), the impedance Z presented by the diode at ω_o is simply $R_S + jX$. According to the preceding section the stability of the network of Fig. 2 can be ascertained from the behavior of $R_S + jX$ using inequality (12), which reduces to

$$R_S \leqq \frac{1}{2} I \left| \frac{dX}{dI} \right| \tag{28}$$

because R_S is independent of I. In order for the network of Fig. 2 to be potentially unstable, inequality (28) must be fulfilled under at least one of the two conditions (14) and (15).

Consider first condition (15), in which case V_{bo} can be assumed independent of I ($V_{bo} \cong V_o$ because $R_S I_o \cong 0$). From eqs. (26) and (27) one obtains

$$\frac{dX}{dI} = \frac{I}{2(C_0\sqrt{\phi})^4\omega_o^3 S_o}. \tag{29}$$

* This power is $\langle 2(Re)V_{bl}e^{j\omega_o t}i_R\rangle_{\text{ave}}$; it can be calculated to a first approximation using eqs. (5), (23), and (27).

Let S_M and S_m denote the maximum and minimum value of $S(t)$. From eq. (22) one can verify that I and S_o are related to S_M and S_m as follows:

$$S_o = \frac{S_M + S_m}{2} \tag{30}$$

$$I = \omega_o(C_o\sqrt{\phi})^2 \frac{S_M - S_m}{2}. \tag{31}$$

These relations and eq. (29) yield

$$I\frac{dX}{dI} = \frac{1}{4}\frac{S_M}{\omega_o}\frac{(1 - S_m/S_M)^2}{(1 + S_m/S_M)} \tag{32}$$

which is valid provided V_{bo} is independent of I.

Now consider condition (14) where V_{bo} is a function of I. In general, no simple relation exists between X and I; however, in Appendix A it is shown that if for a given value of the ratio S_m/S_M the inequality

$$\left|\frac{qv_m}{kT}\right| \gg 1 \tag{33}$$

obtains [v_m is the minimum value of $v_b(t)$], then condition (14) becomes equivalent to

$$S_m = \text{constant} \tag{34}$$

which leads to a simple relation between X and I. In fact, using eqs. (26), (30), and (31), X can be expressed in the form

$$X = -\frac{1}{\omega_o}\left[S_m + \frac{I}{\omega_o(C_o\sqrt{\phi})^2}\right], \tag{35}$$

and X is linearly related to I. Further, using eqs. (31) and (35),

$$I\frac{dX}{dI} = -\frac{S_M - S_m}{2\omega_o}. \tag{36}$$

We now compare the two cases I_o = constant and V_o = constant, under the assumption that in the former case condition (33) is satisfied. From eqs. (32) and (36), for given S_M, S_m, and ω_o, eq. (36) gives a larger magnitude for IdX/dI than eq. (32). Since eq. (36) corresponds to the condition I_o = constant, we conclude that the network of Fig. 2 is potentially unstable only if inequality (28) is fulfilled in that case. From inequality (28) and eq. (36),

$$R_S \leqq \frac{S_M - S_m}{4\omega_o}, \tag{37}$$

which gives the values of R_S, S_M, S_m, and ω_o for which instability (and therefore high gain) is possible. If ω_c denotes the cutoff frequency of the diode, so that $\omega_c = S_M/R_S$, and if $S_m \ll S_M$, then inequality (37) reduces to

$$\omega_c \geqq 4\omega_o \tag{38}$$

which is eq. (1) for $\eta = 4$.

An understanding of the practical validity of inequality (37) is obtained by examining the restrictions in the above analysis. It has been assumed that the voltage across the barrier can be determined to a first approximation by neglecting the barrier resistance and also that the power absorbed at ω_o by the barrier resistance is negligible compared with that dissipated in R_S. These assumptions are certainly satisfied if operation of the diode is restricted to a range of voltages v_b for which the barrier capacitance is predominant over the barrier resistance. However, this restriction is impractical because it would result in a mixer with very poor performance; for optimum performance the diode should be fully pumped; that is, $v_b(t)$ should vary over the entire usable range of forward and reverse voltages. In the following section it is shown that inequality (37) is valid, approximately, even if the diode is fully pumped (in which case the restriction in question is not satisfied), *provided* the breakdown voltage V_B *is sufficiently large.* Thus, we can say that this requirement on V_B [which is in accord with the fact that inequality (37) has been derived under requirement (33)] is the main restriction on inequality (37).

IV. GENERAL CASE

According to eqs. (4) and (5), the voltage and current at the barrier are related through the nonlinear differential equation

$$\frac{C_o\sqrt{\phi}}{\sqrt{\phi - v_b}}\frac{dv_b}{dt} + i_s e^{(q/kT)v_b} - i_s - i_b = 0, \tag{39}$$

with i_b given by eqs. (6) and (7). This equation cannot in general be solved exactly, but an approximate solution can be obtained fairly simply to any degree of accuracy by the Euler method, as shown in Appendix B. Using that method, Z_b, V_{bo}, and their partial derivatives with respect to I_o and I [these derivatives are needed to test the stability of M using inequalities (16) and (17)] have been calculated for various diode characteristics and terminal currents I_o and I. Table I shows

Table I—Four Examples of the Behavior of M

$\frac{i_s e^{(q\phi/kT)}}{C_o\omega_o\sqrt{\phi}} = 31.25 \qquad \frac{I_o + i_s}{C_o\omega_o\sqrt{\phi}} = 0.1$

$\lvert I\rvert/C_o\omega_o\sqrt{\phi}$	0.75	1.00	1.25	1.75
$V_{bo} - \phi$	−0.722	−1.116	−1.603	−2.857
$V_m - \phi$	−1.648	−2.660	−3.919	−7.180
$V_M - \phi$	−0.093	−0.089	−0.086	−0.082
$R_b\cdot\omega_o C_o\sqrt{\phi}$	0.110	0.101	0.096	0.090
$X_b\cdot\omega_o C_o\sqrt{\phi}$	−0.725	−0.904	−1.080	−1.432
$\partial V_{bo}/\partial I_o\cdot\omega_o C_o\sqrt{\phi}$	2.016	2.577	3.133	4.243
$\partial V_{bo}/\partial\lvert I\rvert\cdot\omega_o C_o\sqrt{\phi}$	−1.389	−1.762	−2.134	−2.878
$\partial(\lvert I\rvert R_b)/\partial I_o\cdot\omega_o C_o\sqrt{\phi}$	0.576	0.774	0.966	1.345
$\partial(\lvert I\rvert R_b)/\partial\lvert I\rvert\cdot\omega_o C_o\sqrt{\phi}$	0.0781	0.0763	0.0757	0.075
$\lvert I\rvert\partial X_b/\partial I_o\cdot\omega_o C_o\sqrt{\phi}$	1.403	1.784	2.166	2.937
$\lvert I\rvert\partial X_b/\partial\lvert I\rvert\cdot\omega_o C_o\sqrt{\phi}$	−0.542	−0.710	−0.881	−1.228

four examples where

$$\frac{i_S e^{(q\phi/kT)}}{C_o\omega_o\sqrt{\phi}} = 31.25, \qquad \frac{I_o + i_S}{C_o\omega_o\sqrt{\phi}} = 0.1\ . \tag{40}$$

The four examples correspond to various values of the quantity $I/C_o\omega_o\sqrt{\phi}$, which represents the terminal current at ω_o. The values v_m and v_M in Table I are the minimum and maximum value of $v_b(t)$. Note that according to eq. (20) S_M and S_m are related to v_M and v_m through the relations

$$S_m = \frac{\sqrt{\phi - v_M}}{C_o\sqrt{\phi}}, \qquad S_M = \frac{\sqrt{\phi - v_m}}{C_o\sqrt{\phi}}. \tag{41}$$

One can verify that, in all the four cases of Table I, inequality (16) is violated for $R_S = 0$. Thus, in each case the circuit of Fig. 2 is potentially unstable provided the series resistance R_S is sufficiently small.

The values of R_S associated with potential instability can be derived as follows. In all the cases considered it has been found that if inequality (17) is fulfilled, then inequality (16) is also fulfilled; in other words, if Z satisfies inequality (12) under the condition V_o = constant, then it also satisfies inequality (12) under the condition I_o = constant. This property has already been found to be true in the limiting case discussed in the preceding section. It follows that for the network to be potentially unstable it is necessary (and, of course, sufficient) that $Z = R_S + R_b + jX_b$ satisfy inequality (16). That is, it is necessary that the expression

$$4(R_S + R_b)\left[\left(\frac{\partial(IR_b)}{\partial I}\right) + R_S\right] - I^2\left(\frac{\partial X_b}{\partial I}\right)^2 \tag{42}$$

be nonpositive. This requirement is equivalent to

$$R_S \leqq R_{SC} , \tag{43}$$

where

$$R_{SC} = \frac{1}{2}\left[\sqrt{I\left(\frac{\partial R_b}{\partial I}\right)^2 + I\left(\frac{\partial X_b}{\partial I}\right)^2} - \frac{\partial(IR_b)}{\partial I} - R_b\right] \cdot \tag{44}$$

In fact, one can verify that expression (42) vanishes for $R_S = R_{SC}$ and is negative for $R_S \geqq R_{SC}$. According to inequality (43), R_{SC} is the largest series resistance for which the network of Fig. 2 is potentially unstable.

Figure 4 shows several curves of R_{SC} versus $| v_m - \phi |$ calculated [using Eq. (44)] for different values of $I_o/C_o\omega_o\sqrt{\phi}$ and for $i_s[\exp(q\phi/kT)]/\omega_oC_o\sqrt{\phi} = 31.25$. The four points indicated on the curve relative to $I_o/C_o\omega_o\sqrt{\phi} = 0.1$ correspond to the four cases of Table I, as one can

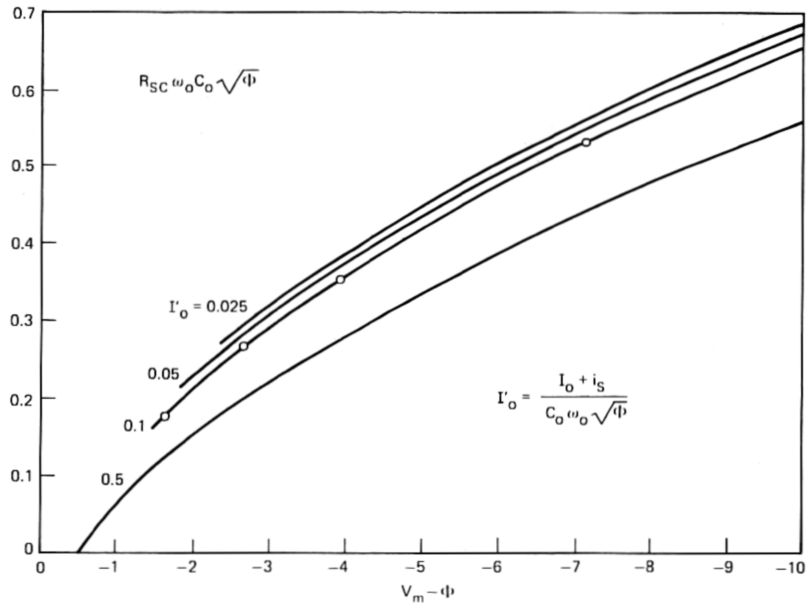

Fig. 4—Behavior of R_{SC} as a function of v_m for different values of I_o.

verify using eq. (44). We see from Fig. 4 that for given diode characteristics and for a given ω_o, the behavior of R_{SC} as a function of I_o and $|v_m - \phi|$ has the following characteristics. For a given I_o, R_{SC} increases monotonically with $|v_m - \phi|$. Since v_m cannot exceed the breakdown voltage, V_B, the largest value of R_{SC} for a given I_o occurs when $v_m = V_B$. For a given v_m, R_{SC} increases with decreasing I_o and approaches a finite limit for $I_o \to 0$. Figure 4 shows that, if $|V_m - \phi| > 2$ volts, R_{SC} is little affected by the value of I_o for $I_o/\omega_o C_o \sqrt{\phi} < 0.1$, approximately.

Now from the discussion of the limiting case of Section III, we know that, if conditions (18) and (33) are satisfied, then according to inequality (37)

$$\frac{R_{SC}\omega_o}{S_M - S_m} = \frac{1}{4}. \tag{45}$$

Condition (18) can be assumed to be fulfilled when $I_o/\omega_o C_o \sqrt{\phi}$ is sufficiently small, in which case the quantity $R_{SC}\omega_o/(S_M - S_m)$ is expected to approach 1/4 for large $|v_m - \phi|$. It is interesting to compare this asymptotic behavior of $R_{SC}\omega_o/(S_M - S_m)$ with the behavior corresponding to the curves of Fig. 4. Figure 5 shows $R_{SC}\omega_o/(S_M - S_m)$ plotted as a function of $|v_m - \phi|$ for the four cases corresponding to

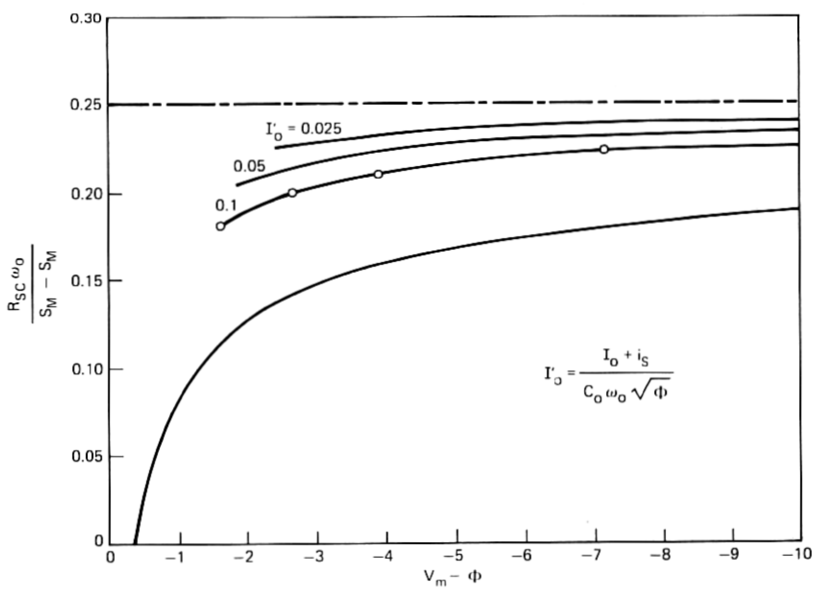

Fig. 5—Behavior of $R_{SC}\omega_o/(S_M - S_m)$.

the curves of Fig. 4. One sees that $R_{SC}\omega_o/(S_M - S_m)$ never exceeds 1/4, and that if $I_o/\omega_o C_o\sqrt{\phi}$ is sufficiently small, $R_{SC}\omega_o/(S_M - S_m)$ approaches 1/4 for large $|v_m - \phi|$, as expected. The four points indicated in Fig. 5 correspond to the cases of Table I.

So far, the quantity $i_S[\exp(q\phi/kT)]/\omega_o C_o\sqrt{\phi}$ has been assumed to be 31.25; Fig. 6 shows how $R_{SC}/\omega_o C_o\sqrt{\phi}$ is affected if $i_S[\exp(q\phi/kT)]/\omega_o C_o\sqrt{\phi}$ is changed from 31.25 to 1.08. The two curves of Fig. 6 have been calculated for $I_o/\omega_o C_o\sqrt{\phi} = 0.1$. It is evident that $R_{SC}/\omega_o C_o\sqrt{\phi}$ does not depend critically on the value of $i_S/\omega_o C_o\sqrt{\phi}$. The four points indicated in Fig. 6 correspond to the four cases of Table I.

4.1 *Region of Instability for Typical Diode Characteristics*

Typically, the breakdown voltage is sufficiently large so that one can assume $\phi - v_m > 2$ volts. For such values of $\phi - v_m$ one can verify from Fig. 4 that $R_{SC}\omega_o C_o\sqrt{\phi}/\sqrt{\phi - v_m} > 0.16$ if $I_o/\omega_o C_o\sqrt{\phi} < 0.5$. Thus, one can assume for typical diodes

$$0.16 < \frac{R_{SC}\omega_o C_o\sqrt{\phi}}{\sqrt{\phi - v_m}} < 0.25. \tag{46}$$

In the introduction, the range of pump frequencies associated with potentially unstable behavior was expressed in terms of the parameter η. A comparison of inequalities (1) and (43) shows that this parameter is

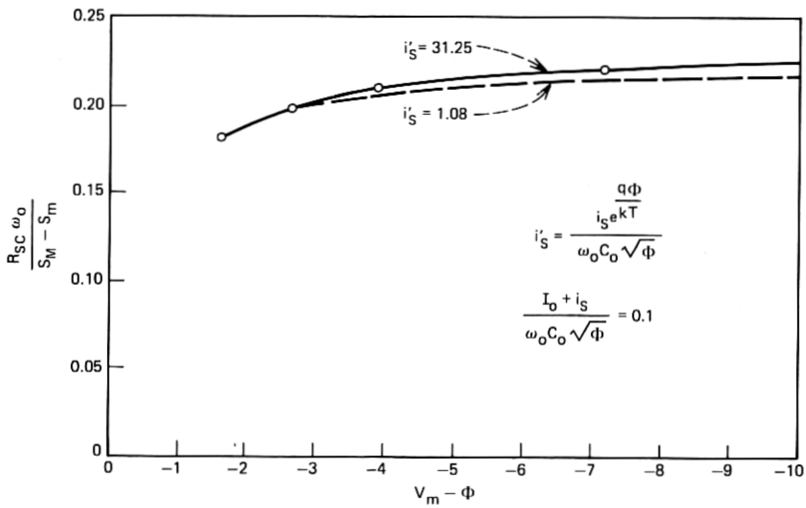

Fig. 6—Effect of i_S.

related to R_{SC} as follows:

$$\eta = \frac{\omega_c}{\omega_o}\frac{R_S}{R_{SC}} = \frac{S_M}{\omega_o R_{SC}} = \frac{\sqrt{\phi - v_m}}{R_{SC}\omega_o C_o \sqrt{\phi}}. \tag{47}$$

Thus, according to inequality (46), η typically lies between 4 and 6.25, as was stated in the introduction.

V. EFFECT OF R_S ON NOISE PERFORMANCE AT HIGH GAIN

The limit imposed by R_S on the optimum noise performance obtainable at high gain is now derived, when the diode is used as a down-converter and is terminated with equal impedances at $\omega_o \pm p$. The effect of R_S on noise can be separated into two parts: one is the effect at $\omega_o \pm p$, and the other at the output frequency p. We will see that if the diode is operated at high gain, the effect at $\omega_o \pm p$ is minimized when the diode is terminated with a very high impedance at $\omega = p$. Under this condition the effect of R_S at $\omega = p$ vanishes and can therefore be ignored.

Consider the effect of R_S at $\omega_o \pm p$. If R_α denotes the real part of the equal terminations at $\omega_o + p$ and $\omega_o - p$, the real part of the total impedance terminating the barrier at $\omega_o \pm p$ is $R_{\alpha t} = R_\alpha + R_S$. Now inequality (43) implies that high gain is possible only if $R_{\alpha t} \leqq R_{SC}$, that is, only if

$$R_\alpha \leqq R_{SC} - R_S . \tag{48}$$

Furthermore, when the resistance $R_{\alpha t}$ equals R_{SC} (i.e., when $R_\alpha = R_{SC} - R_S$), one can show that high gain requires a very high output impedance in all cases of Section IV. (This is a direct consequence of the fact that, when the resistance seen by the barrier at ω_o equals R_{SC}, instability may arise only if I_o = constant; that is, only if the diode is biased by a dc supply with infinite internal impedance.)

Now the ratio of the thermal noise power available (at $\omega_o \pm p$) at the barrier to that available at the terminals of the diode is $R_{\alpha t}/R_\alpha$. This represents the impairment caused by the presence of R_S at $\omega_o \pm p$ on the noise performance of the diode as a down-converter. According to inequality (48), this impairment is minimized when R_α equals $R_{SC} - R_S$, in which case a very high termination is required at $\omega = p$. Thus, since the effect of R_S at $\omega = p$ vanishes, and at $\omega = \omega_o \pm p$ is given by the ratio $R_{SC}/(R_{SC} - R_S)$, the noise figure can be written

$$F_m = \frac{R_{SC}}{R_{SC} - R_S} F, \tag{49}$$

where F is the noise figure obtainable at high gain in the ideal case $R_S = 0$, when the termination at $\omega = p$ is a very high impedance. Using eq. (47) this relation can be rewritten

$$F_m = \left(1 - \eta \frac{\omega_o}{\omega_c}\right)^{-1} F \tag{50}$$

from which one obtains inequality (3).

VI. EXPERIMENTAL RESULTS*

Experimental data have been obtained at a pump frequency of 1.25 GHz using a GaAs Schottky barrier diode,† having $R_S \cong 4$ ohms, $C_o \cong 1.2$ pF, and $V_B \cong 10$ volts. This diode was mounted in a circuit designed to produce at the barrier very high terminating impedances at $2\omega_o$, $3\omega_o$, and $4\omega_o$. The structure is shown in Fig. 7 with the cover plate removed; the diode is inserted between two resonators both of which operate in the TEM mode. One resonator is connected to a 50-ohm coaxial line and consists of a main line with two series-resonant circuits connected in shunt. The purpose of the two series-resonant circuits is to short out transmission at $2\omega_o$ and $4\omega_o$ between the 50-ohm coaxial line and the diode. Each circuit consists of a line element connected to the main line at one end, with a lumped capacitance between the other end of each line element and ground.

The main line has the diode chuck soldered at one end; the other end is open-circuited. The electrical distance between the open-circuited end and the connection point at which the coaxial line is attached is a quarter of a wavelength at $3\omega_o$. The connection point of the coaxial line is therefore also short-circuited at $3\omega_o$. The distance from this connection point to the diode and the dimensions of the other resonator were chosen so as to open-circuit the barrier of the diode at $2\omega_o$, $3\omega_o$, and $4\omega_o$, using the following procedure. Initial dimensions for the two resonators were obtained experimentally by adjusting one resonator at the time (the other resonator and the diode being removed). The L-shaped resonator was adjusted so as to obtain two resonances at $2\omega_o$ and $4\omega_o$. The other resonator was adjusted (with the 50-ohm line terminated in 50 ohms) for a resonance at $3\omega_o$. Then an empty package identical to that of the diode used in this experiment was mounted between the two resonators as shown in Fig. 7, and the resonant frequencies of this circuit were measured by coupling the circuit

* The experiment described in this section was carried out by S. Michael of Bell Laboratories.

† Supplied by J. C. Irvin of Bell Laboratories.

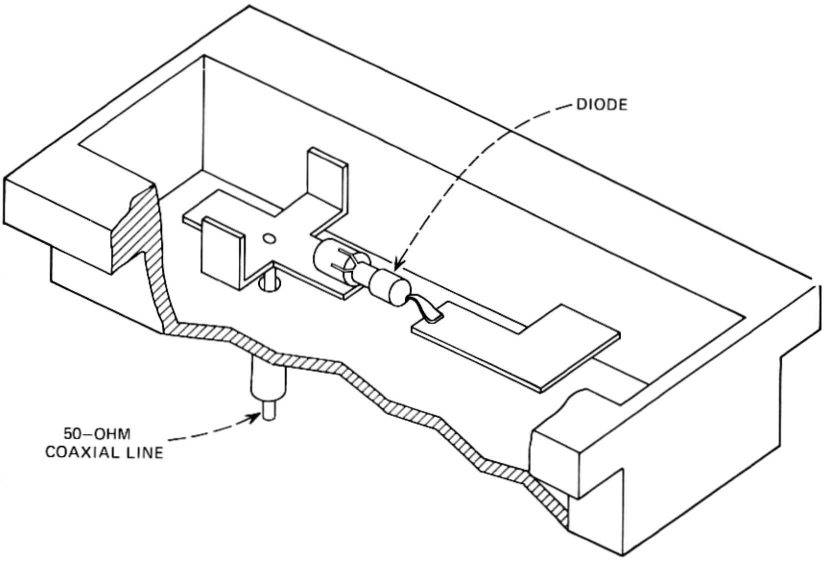

Fig. 7—Circuit used to open-circuit the barrier of the diode at $2\omega_o$, $3\omega_o$ and $4\omega_o$.

to a load and a generator by means of two loosely coupled capacitive probes. The resonant frequencies were found to be appreciably different from $2\omega_o$, $3\omega_o$, and $4\omega_o$ as expected, because of the coupling between the two resonators resulting from the case capacitance of the package. The dimensions of the two resonators were then adjusted to give the desired resonances at $2\omega_o$, $3\omega_o$, and $4\omega_o$ and the empty package was finally replaced with the actual diode.

In order to separate the pump frequency ω_o from dc, the 50-ohm coaxial line of the circuit of Fig. 7 was connected to one of the three arms of a monitor tee consisting of a main line shunted by an auxiliary line. The two lines are provided with a capacitor and an inductor connected in series to their central conductors to block signals in the vicinity of dc and ω_o, respectively. The other two arms of the monitor tee are connected to an output matching network and a tuner, as shown schematically in Fig. 8.

Figure 9 shows a block diagram of the apparatus used to measure the noise characteristics of the mixer of Fig. 8. The noise source is the AIL type 70 Hot-Cold Body Standard Noise Generator [consisting of two terminations, one immersed in liquid nitrogen (77.3°K) and the other mounted in a temperature-controlled oven (373.2°K)]. The pump is connected to a narrowband filter. This filter consists of four identical

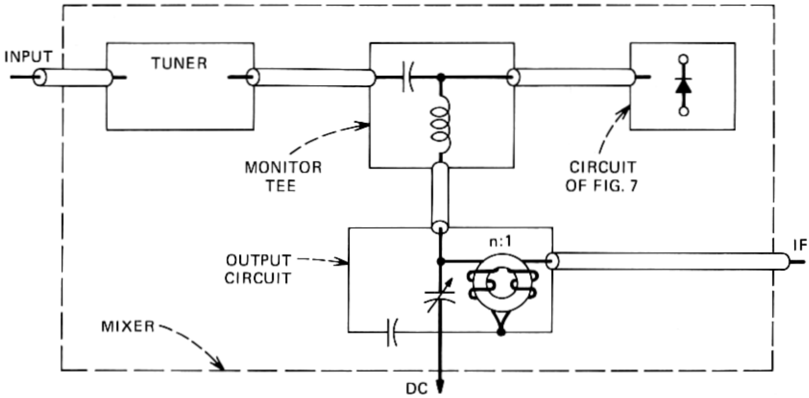

Fig. 8—Mixer.

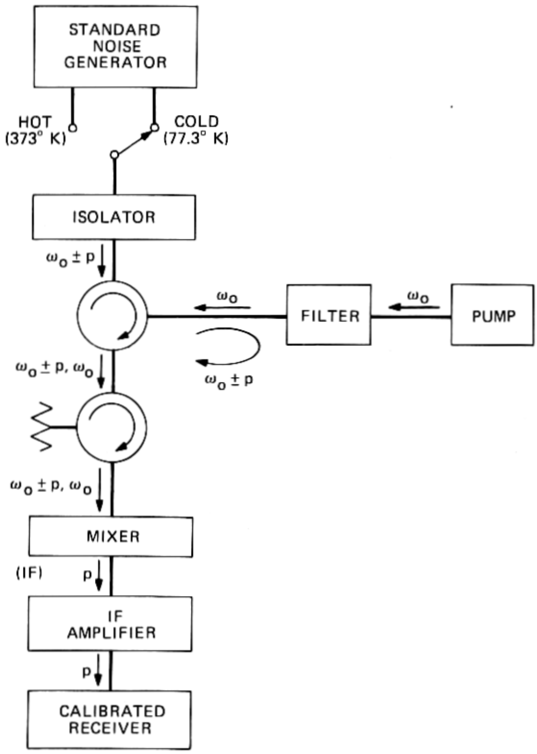

Fig. 9—Block diagram of apparatus used to test the mixer of Fig. 8; $\omega_o = 1.25$ GHz; $p = 2$ MHz.

cavity resonators tuned at ω_o and separated by transmission lines $\lambda/4$ long at ω_o; the attenuation at ω_o is approximately 10 dB and, at $\omega_o \pm p$ for $p \geqq 2$ MHz, is greater than 55 dB; its fractional bandwidth is approximately 0.07 percent. The noise source is buffered by an isolator providing more than 22 dB isolation at $\omega_o \pm p$. The noise components originating from the source at $\omega_o \pm p$ ($p \geqq 2$ MHz) enter the first circulator and are directed into the pump filter which reflects them back to the circulator where they are directed into a second circulator. The second circulator, which provides 22 dB of isolation at $\omega_o \pm p$, is followed by the mixer, the circuit of which is shown in Figs. 8 and 9. The noise power entering the mixer at $\omega_o \pm p$ is converted to the output (IF) frequency $p \cong 2$ MHz. The converted power is then amplified and finally measured with a narrowband receiver. The IF amplifier system consists of a calibrated variable attenuator followed by an amplifier, the noise figure of which was optimized at 0.19 dB for $p = 2$ MHz. The purpose of the variable attenuator is to vary the noise figure F_i of the IF amplifier.

The double-sideband noise figure of the mixer-amplifier combination is given by the familiar relation

$$F_r = F_m + \frac{F_i - 1}{G_m}, \tag{51}$$

where F_m is the double-sideband noise figure of the mixer* and G_m is its gain. Note that G_m is not the conversion gain from $\omega_o + p$ to p, or from $\omega_o - p$ to p, but is the *sum* of the two. That is, if $G_{\alpha\beta}$ and $G_{\gamma\beta}$ denote these two gains, $G_m = G_{\alpha\beta} + G_{\gamma\beta}$ (thus $G_m \cong 2G_{\alpha\beta}$ because $G_{\alpha\beta} \cong G_{\gamma\beta}$). Measurement of F_r consists essentially of determining two quantities: (*i*) the ratio $Y = P_2/P_1$, where P_2 and P_1 are the power outputs of the IF amplifier corresponding to the two temperatures $T_2 = 373.2$°K and $T_1 = 77.3$°K and (*ii*) the insertion loss ℓ of the circuit connected between the source and the mixer; this loss is less than 1 dB and can be measured very accurately. The noise figure is given by the well-known formula $F_r = [1 + (T_2 - T_1Y)/290(Y - 1)]\ell$. The accuracy of measurement of F_r is limited primarily by the accuracy of the two temperatures T_2 and T_1; the estimated error for F_r is less than 0.1 dB.

According to eq. (51), F_m and G_m can be determined indirectly by measuring the effects of F_r of varying the IF noise figure F_i. Figure 10 shows a plot of F_r versus F_i which was obtained after adjusting the

* F_m is the ratio of the total noise power output of the mixer to that portion of this power originating from the terminations of the mixer at $\omega_o + p$ and $\omega_o - p$, assuming these terminations are at 290°K.

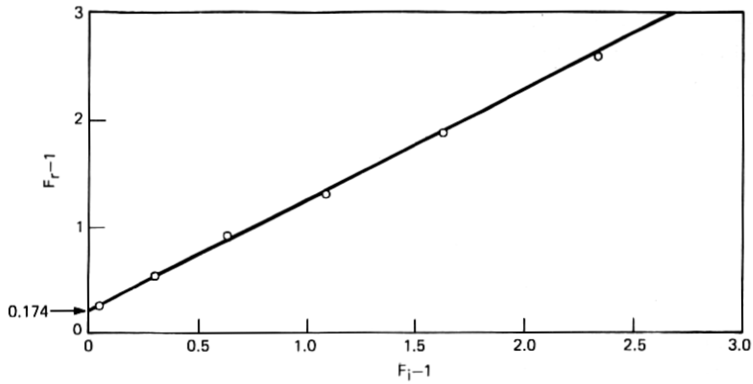

Fig. 10—Behavior of F_r versus F_i; mixer optimized for $F_i = 0.19$ dB.

mixer for minimum F_r under the particular condition $F_i = 0.19$ dB. According to eq. (51) the slope of this curve is the mixer conversion loss $L_m = 1/G_m$ and the point corresponding to $F_i = 1$ is F_m. This curve tells us that for a gain of 0.948 the lowest noise figure obtainable from the mixer is 1.174.

Figure 11 shows a plot of the minimum noise figure of the mixer versus its conversion loss. From this plot we can derive the lowest F_r obtainable for a given F_i as follows. From eq. (51), after replacing $1/G_m$ with L_m and differentiating, we get

$$\frac{dF_r}{dL_m} = \frac{dF_m}{dL_m} + (F_i - 1) \cdot \tag{52}$$

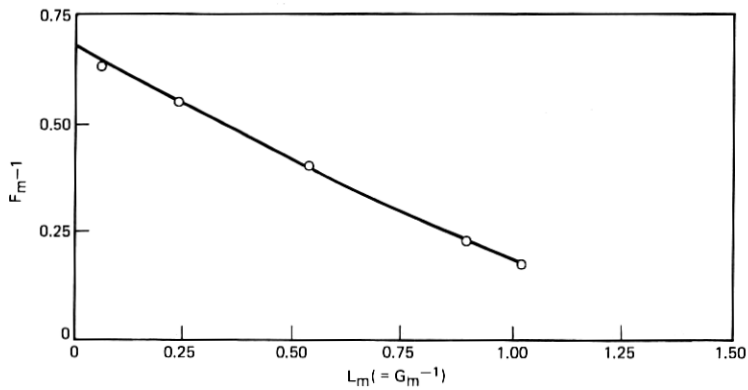

Fig. 11—Behavior of F_m versus $L_m = G_m^{-1}$.

Because the curve of Fig. 11 has $d^2F_m/d^2L_m > 0$, it follows that a point on the curve minimizes F_r if it satisfies $dF_r/dL_m = 0$ which, from eq. (52), results in

$$F_i = 1 - \frac{dF_m}{dL_m} \cdot \tag{53}$$

Using this equation, we obtain from Fig. 11 the curve of Fig. 12, which shows the relation between F_i and the optimum value of L_m. One sees that it is desirable to have $L_m < 1$ (i.e., gain greater than unity) when

$$F_i > 1.37 \ (\sim 1.4 \text{ dB}) \ . \tag{54}$$

VII. CONCLUSIONS

It has been shown that a Schottky barrier diode is capable of arbitrarily high conversion gain as a mixer provided $\omega_o < \omega_c/\eta$, where η is a parameter typically less than 6.25, but always greater than 4. If $\omega_o \ll \omega_c/\eta$, then according to inequality (3), the ultimate double-sideband noise figure at high gain should be very close to unity. A fortiori, the ultimate noise figure at low gain should be excellent, if $\omega_o \ll \omega_c/\eta$. These conclusions are corroborated by the experimental results. Although the experimental result obtained is very good (F_m, 0.7 to 2.3 dB), it does not achieve the theoretical limit, nor was it expected to; practical limitations such as input circuit losses, estimated to exceed 0.4 dB for $G_m \gg 1$, confine the experimental noise figure for $G_m \gg 1$ to values appreciably higher than the theoretical limit.

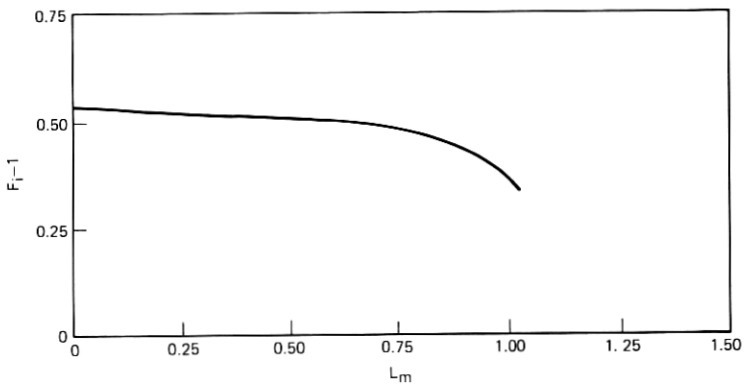

Fig. 12—Relation between F_i and the optimum value of L_m.

VIII. ACKNOWLEDGMENTS

The author is indebted to D. C. Hogg for his help and guidance in the preparation of this paper. Thanks are also expressed to C. L. Ruthroff for a number of useful discussions during the course of the work.

APPENDIX A

In this appendix, we analyze the condition I_o = constant for the case of $|(qv_m/kT)| \gg 1$ of Section III. The average current through the barrier resistance is

$$I_o = \langle i_s e^{(q/kT)v_b(t)} \rangle_{\text{ave}} - i_s \, . \tag{55}$$

Thus, if a perturbation δI is applied to the diode current at ω_o, while I_o is held constant, from eq. (55) the resulting perturbation of $v_b(t)$ must satisfy the condition

$$\langle e^{+(q/kT)v_b(t)} \ \delta v_b(t) \rangle_{\text{ave}} = 0. \tag{56}$$

According to eq. (20) this condition can be rewritten in the form

$$\langle e^{-BS^2(t)} S(t) \ \delta S(t) \rangle_{\text{ave}} = 0, \tag{57}$$

where

$$B = \frac{q}{kT} (C_o \sqrt{\phi})^2. \tag{58}$$

Note that $S(t)$ is completely specified by its maximum and minimum value S_M and S_m. We will presently show that if for a given value of the ratio

$$r = \frac{S_m}{S_M} \tag{59}$$

we let $S_M \to \infty$ then the time function $\exp[-BS^2(t)]$ over the interval $-T/2 \leqq t \leqq T/2$ approaches an impulse located at $t = 0$. Thus, if A denotes the area of this impulse, we will show that for a given value of r we can write:

$$\exp[-BS^2(t)] \to Au_o(t) \qquad (|\, t\, | \leqq T_o/2) \tag{60}$$

for $S_M \to \infty$, where $u_o(t)$ denotes the unit impulse. From this result and the fact that $S(0) = S_m$ we find that for $S_M \to \infty$ Eq. (56) becomes

$$S(0) \ \delta S(0) = S_m \ \delta S_m = 0. \tag{61}$$

We can thus say that for $S_M \to \infty$, condition (14) is equivalent to condition (34). We now show that relation (60) is true for $S_M \to \infty$.

Let ϵ be an arbitrarily small positive quantity. We have to show that for a given value of r

$$\lim_{S_M \to \infty} \frac{\int_\epsilon^{T/2} \exp\,[-BS^2(t)]\,dt}{\int_0^{T/2} \exp\,[-BS^2(t)]\,dt} = 0\,. \tag{62}$$

First, note that $S(t)$ can be written

$$S(t) = S_M\left[\frac{1+r}{2} - \frac{1-r}{2}\cos\omega_o t\right]. \tag{63}$$

Using this expression one can verify that $\exp\,[-BS^2(t)] < \exp\,[-BS^2(\epsilon)]$ for $\epsilon < t \leqq T/2$. Thus,

$$\int_\epsilon^{T/2} \exp\,[-BS^2(t)]\,dt < \frac{T}{2}\exp\,[-BS^2(\epsilon)]\,. \tag{64}$$

Furthermore, it can be shown that if $S_M B$ is sufficiently large then

$$\int_0^{T/2} \exp\,[-BS^2(t)]\,dt > \frac{T}{2}\,\frac{e^{-r^2 S_M{}^2 B}}{\sqrt{2\pi r(1-r)BS_M^2}}\,. \tag{65}$$

In fact, since $\cos\omega_o t > 1 - (\omega_o t)^2/2$, from eq. (63)

$$\begin{aligned} S^2(t) &< S_M^2\left[r + \frac{(1-r)}{4}(\omega_o t)^2\right]^2 \\ &= S_M^2\left[r^2 + \frac{(1-r)r}{2}(\omega_o t)^2 + \frac{(1-r)^2}{16}(\omega_o t)^4\right]. \end{aligned}$$

This inequality allows one to write

$$\begin{aligned} &\int_0^{T/2} \exp\,[-BS^2(t)]\,dt \\ &\quad > \frac{T}{2\pi}\,\frac{e^{-r^2 S_M{}^2 B}}{\sqrt{r(1-r)BS_M^2/2}}\int_0^{\pi\sqrt{r(1-r)BS_M{}^2/2}} \exp\,[-u^2 - \gamma u^4]\,du, \end{aligned}$$

where $\gamma = (4BS_M^2 r^2)^{-1}$. If BS_M is sufficiently large, so that $\gamma \ll 1$, then from this inequality we obtain (65).

From inequalities (64) and (65) we obtain

$$\frac{\int_\epsilon^{T/2} \exp\,[-BS^2(t)]\,dt}{\int_0^{T/2} \exp\,[-BS^2(t)]\,dt} < \sqrt{2\pi BS_M^2(1-r)r}\; e^{-B[S^2(\epsilon) - r^2 S_M{}^2]}. \tag{66}$$

According to Eq. (63) we can write

$$S^2(\epsilon) - r^2 S_M^2 = S_M^2 \mathcal{E}_r(\epsilon), \tag{67}$$

where $\mathcal{E}_r(\epsilon)$ is a positive quantity which depends upon r and ϵ, but is independent of S_M. From eq. (67) and inequality (66) we therefore conclude that eq. (62) is true. Note that, since ϵ is a small quantity, from eqs. (63) and (67) we can write

$$\mathcal{E}_r(\epsilon) \cong \frac{(1 - r)r\epsilon^2}{2}.$$

Thus,

$$\frac{\int_\epsilon^{T/2} \exp\,[-BS^2(t)]\,dt}{\int_0^{T/2} \exp\,[-BS^2(t)]\,dt} \ll 1$$

provided

$$BS_M^2 \gg \frac{2}{(1 - r)r\epsilon^2}.$$

APPENDIX B

Figure 13 shows a network consisting of a variable elastance, a variable resistance, and a constant resistance R'_s. Assume that the current i'_R through the variable resistance is related to the voltage v'_b as follows:

$$i'_R = i'_S e^{qv_b'/kT} \tag{68}$$

and that the variation of the elastance S' is characterized by the relation

$$S' = \sqrt{-v'_b}\,. \tag{69}$$

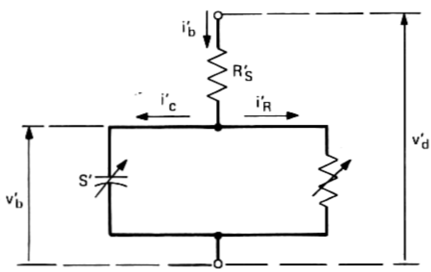

Fig. 13—Network representing a Schottky barrier diode.

Let the terminal current i_b' of this network be a periodic function of τ with period 2π, so that

$$i_b' = i_b'(\tau) = i_b'(\tau + 2\pi) \,. \qquad (70)$$

Then, i_b' and v_b' are related through the differential equation

$$\frac{1}{\sqrt{-v_b'}}\frac{dv_b'}{d\tau} + i_s'e^{(q/kT)v_b'} - i_b' = 0. \qquad (71)$$

Furthermore, one sees from Fig. 13 that the terminal voltage v_d' can be written

$$v_d' = i_b'R_s' + v_b' \,. \qquad (72)$$

A Schottky barrier diode can always be represented by such a network. In fact, if we assume

$$\begin{aligned}
\tau &= \omega_o t \\
v_b' &= v_b - \phi, \qquad v_d' = v_d - \phi + i_s R_s \\
i_s' &= \frac{i_s e^{(q\phi/kT)}}{C_o\omega_o\sqrt{\phi}} \\
i_b' &= \frac{i_b}{C_o\omega_o\sqrt{\phi}} + \frac{i_s}{C_o\omega_o\sqrt{\phi}} \\
R_s' &= R_s\omega_o C_o\sqrt{\phi} \qquad (73)
\end{aligned}$$

and substitute these relations in eqs. (71) and (72), we obtain eq. (39) and the relation $v_d = i_b R_s + v_b$. Thus, the two networks of Figs. 11 and 13 are equivalent.

Analysis

Let us now assume for i_b' the form

$$i_b' = i_b'(\tau) = \begin{cases} C, & \text{for} \quad \tau \leqq 0 \\ I_o' + 2I'\cos\tau, & \text{for} \quad \tau > 0 \end{cases} \qquad (74)$$

where C is a constant. Since then $i_b' = i_R' = C$ for $\tau \leqq 0$, from eq. (68):

$$v_b' = v_b'(\tau) = \frac{kT}{q}(\ln C - \ln i_s') \quad \text{for} \quad \tau \leqq 0. \qquad (75)$$

Since for $\tau \geqq 0$, $i_b'(\tau)$ is periodic, it is reasonable to expect that for τ sufficiently large, $v_b'(\tau)$ will also be periodic. Let us suppose there is a positive integer N such that one can write to a good approximation

$$v'_b(2\pi N + 2\pi) \cong v'_b(2\pi N), \tag{76}$$

so that $v'_b(\tau)$ can be assumed to be periodic for $\tau \geqq 2\pi N$,

$$v'_b(\tau + 2\pi) \cong v'_b(\tau), \quad \text{for} \quad \tau \geqq 2\pi N. \tag{77}$$

Then we can write

$$v'_b(\tau) \cong v'_{bo} + 2(\mathrm{Re})(v'_{b1}e^{i\tau} + \cdots) \quad \text{for} \quad \tau \geqq 2\pi N, \tag{78}$$

where the dots indicate the components of order 2, 3, etc., and

$$V'_{bo} = \frac{1}{2\pi} \int_{2\pi N}^{2\pi N + 2\pi} v'_b(\tau)\, d\tau \tag{79}$$

and

$$V'_{b1} = \frac{1}{2\pi} \int_{2\pi N}^{2\pi N + 2\pi} v'_b(\tau) e^{-i\tau}\, dt\,. \tag{80}$$

Thus, if we can determine the behavior of $v'_b(\tau)$ over the interval $2\pi N \leqq \tau \leqq 2\pi(N + 1)$, where N is the smallest positive integer for which condition (76) can be assumed to be fulfilled, then the coefficients V'_{bo} and V'_{b1} can be readily determined by these two relations.

For given values of C, I'_o and I', an approximate solution to eq. (71) can be obtained using the Euler method. This method requires that the continuous variable τ be replaced by the discrete variable $n\tau_o$ ($n = 0$, ± 1, ± 2, etc.). Since in eq. (74) for $\tau \geqq 0$ $i'_b(\tau)$ has period 2π, it is convenient to assume for the step size τ_o an exact submultiple of 2π,

$$\tau_o = \frac{2\pi}{P} \tag{81}$$

where P is a positive integer. In the Euler method of solution, eq. (71) is replaced by the difference equation

$$v'_{n+1} = v'_n + D_n\tau_o\,, \tag{82}$$

where v'_n is the approximation to v'_b for $\tau = n\tau_o$, and D_n is the approximation to the derivative $dv'_b/d\tau$ for $\tau = n\tau_o$. From eq. (71)

$$D_n = \sqrt{-v'_n}\,(i'_n - i'_s e^{(q/kT)v_n'}) \tag{83}$$

where

$$i'_n = \begin{cases} I'_o + 2I' \cos(n\tau_o), & \text{for} \quad n > 0 \\ C, & \text{for} \quad n = 0 \end{cases}. \tag{84}$$

Equations (82) to (84) show that the values of v_o, v_1, v_2, etc. can be calculated sequentially, starting with

$$D_o = 0, \qquad v_o' = \frac{kT}{q} \ln \left(\frac{i_o'}{i_s'} \right), \tag{85}$$

then calculating v_1' and D_1, and so on. Let N be the smallest integer for which the condition

$$v'_{P(N+1)} = v'_{PN} \tag{86}$$

is satisfied. Then, according to eqs. (79) and (80) the desired approximations to V_o' and V' are

$$\begin{aligned} V_o' &= \frac{1}{P} \sum_{K=0}^{P-1} v'_{K+PN} \\ V_o' &= \frac{1}{P} \sum_{K=0}^{P-1} v'_{K+PN} e^{-i\tau}{}_{K+PN} . \end{aligned} \tag{87}$$

Table I* and Figs. 4 to 6 have been calculated choosing as initial condition

$$i_0' = C = I_0' + 2I'. \tag{88}$$

The value of N depends on the value of I_0'. One can show that $N \to \infty$ for $I_0' \to 0$. Thus, the above method is not suitable if I_0' is too small. However, for the values of I_0' that are of practical interest, N is typically a small integer; for instance, $N \leqq 4$ in all the cases in Table I.

REFERENCES

1. Watson, H. A., *Microwave Semiconductor Devices and Their Circuit Applications*, New York: McGraw-Hill, 1969.
2. Abele, T. A., Alberts, A. J., Ren, C. L., and Tuchen, G. A., "Schottky Barrier Receiver Modulator," B.S.T.J., *47*, No. 7 (September 1968), pp. 1257–1287.
3. Elder, H. E., et al., "Active Solid-State Devices," B.S.T.J., *47*, No. 7 (September 1968), pp. 1323–1375.
4. Osborne, T. L., Kibler, L. U., Snell, W. W., "Low Noise Receiving Down-Converter," B.S.T.J., *48*, No. 6 (July–August 1969), pp. 1651–1663.
5. Dragone, C., "Amplitude and Phase Modulation in Resistive Diode Mixers," B.S.T.J., *48*, No. 6 (July–August 1969), pp. 1967–1997.
6. Dragone, C., "Conditions of High Gain in Mixers and their Relation to the Jump Phenomenon," B.S.T.J., this issue, pp. 2139–2167.
7. Torrey, H. C., and Whitmer, C. A., *Crystal Rectifiers*, *15*, Rad. Lab. Series, New York: McGraw-Hill, 1948.

* Note that according to eqs. (73) the various expressions of Table I have the following significance: $(I_o + i_s)/C_o\omega_o\sqrt{\phi} = I_o'$; $I/C_o\omega_o\sqrt{\phi} = I'$; $V_{bo} - \phi = V_{bo}'$; $V_m - \phi$ and $V_M - \phi$ are the minimum and maximum value of $v_b(\tau)$; $Z_b\omega_oC_o\sqrt{\phi} = Z_b' = V_{b1}'/I'$; etc.

8. Edwards, C. F., "Frequency Conversion by Means of a Nonlinear Admittance," B.S.T.J., *35*, No. 6 (November 1956,) pp. . 1403–1416.
9. MacPherson, A. C., "An Analysis of the Diode Mixer Consisting of Nonlinear Capacitance and Conductance and Ohmic Spreading Resistance," *IRE Trans. MTT*, *MTT-5* (January 1957), pp. 43–51.
10. Engelbrecht, R. S., "Parametric Energy Conversion by Nonlinear Admittances," Proc. IRE, No. 50 (March 1962), pp. 312–320.
11. Becker, L., and Ernst, R. L., "Nonlinear-Admittance Mixers," RCA Rev., *25* (December 1964), pp. 662–691.
12. Liechti, C. A., "Down-Converters Using Schottky-Barrier Diodes," IEEE Trans. Electron Devices, *ED-17*, No. 11 (November 1970), pp. 975–983.